ELSEVIER

Ceramics International 31 (2005) 917–922

CERAMICS INTERNATIONAL

www.elsevier.com/locate/ceramint

Processing of mullite–zirconia grains for slip cast ceramics

F. Temoche[1], L.B. Garrido[1,*], E.F. Aglietti[2]

Centro de Tecnología de Recursos Minerales y Cerámica (CETMIC), Cno. Centenario y 506. C.C.49 (B1897 ZCA), M.B. Gonnet. Prov. de Buenos Aires, Argentina

Received 30 July 2004; received in revised form 1 August 2004; accepted 2 October 2004
Available online 21 January 2005

Abstract

Dense composites were prepared by slip casting and sintering at 1600 °C from a commercially available mullite–zirconia powder which was finely ground in an attrition mill. Submicron alumina and a mixture of alumina and zircon were used as sintering aids. The effects of amount of dispersant and pH on colloid stability of diluted suspensions were determined to obtain the optimum conditions for suspension stabilization. The influence of powder composition and solid content on flow behavior of concentrated suspensions and on density of green cast were analyzed. Dried compacts achieved a relative density nearly to 60% theoretical density (TD) for fused zirconia mullite powder with and without 10 wt.% of sintering aids. Density, microstructure and crystalline phase content of sintered compacts such as were determined and analyzed in relation to the previous processing.

Keywords: A. Slip casting; D. Mullite; D. Zirconia; Processing

1. Introduction

Mullite and zirconia are widely used as components in ceramic materials because of their excellent resistance to creep and spalling, and high mechanical strength.

Mullite–zirconia–alumina refractories are used in the forehead feeders and glass melting furnaces as glass contact material such as plungers, spouts, tubes, orifice rings, etc. [1,2]. The wide spread use of this class of materials is due to their high corrosion resistance attributed to the microstructure and to zirconia being slightly wetted by siliceous and metallic melts. Since the solubility potential of zirconia in silica is low, the chemical attack of the refractory is comparatively low [3].

Mullite–zirconia ceramics can be obtained by mixing and reacting suitable mixtures of zircon raw material and alumina. Mullite–zirconia grains are offered as raw material to elaborate ceramics and refractories, this powder consisting in mullite and m-ZrO_2 as principal crystalline phases.

Generally, the materials are produced by sintering of a green body elaborated by conventional dry preparation methods [4–6]. However, a variety of processing techniques may be applied [7,8]. Slip casting is considered a successful method to improve density and microstructure of the body so this technique is applied in the fabrication process of many composites and refractories.

To achieve improvements in the density and microstructure of the consolidate the colloidal stability and rheological behavior must be controlled. Control or manipulation of the interparticle colloidal forces by adjusting the pH or by adding dispersant is generally used to improve the properties of suspension which, in turn, improve the resulting properties of the green and sintered material. Well-dispersed suspensions can be packed at high relative density without large pores or agglomerates.

In this work, slip casting was used as consolidation method to obtain dense mullite–zirconia composite from a fused mullite–zirconia powder which was finely ground in an attrition mill. The addition of alumina and a mixture of alumina and zircon were used to enhance sintering

* Corresponding author.
E-mail address: lgarrido@cetmic.unlp.edu.ar (L.B. Garrido).
[1] CONICET.
[2] CONICET-UNLP.

0272-8842/$30.00
doi:10.1016/j.ceramint.2004.10.005

Table 1
Phase composition determined by the Rietveld method

Material	T (°C)	Mullite (wt.%)	m-ZrO_2 (wt.%)	t-ZrO_2 (wt.%)	Al_2O_3 (wt.%)	$ZrSiO_4$ (wt.%)
As-received MZ	–	60	39	–	–	1
Milled MZ	–	50	49	–	1	Traces
Sintered MZ	1600	49	44	3	3	Traces
Sintered MZa	1600	56	39	3	2	Traces
Sintered MZaz	1600	52	44	2	2	Traces

properties. Dried and sintered density of compacts that were consolidated by slip casting were correlated with rheological properties of the suspensions and their compositions.

2. Materials and methods

2.1. Starting materials

The fused mullite–zirconia powder (MVZr, Elfusa, Brasil) having a large mean particle size d_{50} of 10 μm was attrition milled (40 h at 400 rpm in water with zircon balls 1.5 to 2 mm in diameter). Prior to milling the as-received MVZr powder was fractionated using sedimentation to obtain the <10 μm fraction. Table 1 shows the crystalline phase composition of the as-received and milled powders determined by XRD.

Mixes consisting in milled MZ powder and 10 wt.% of alumina (MZa) and 10 wt.% a mixture of alumina and zircon (MZaz) were prepared. α-Alumina (A-16 SG, Alcoa Inc., USA) powder with a mean particle size of 0.4 μm and a BET surface area of 9.5 m^2/g was used. Zircon (Mahlwerke Kreutz, Mikron, Germany) powder was characterized by a large mean particle size (2 μm) and 4 m^2/g BET surface area. The alumina/zircon (wt.%) ratio of the mixture was 45.5/54.5 that corresponds to the alumina/zircon molar ratio of 1.5 (stoichiometric 3:2) to produce mullite and zirconia after reaction at temperatures close to 1600 °C.

Average particle size d_{50} (Sedigraph 5000D, Micromeritics) was used to evaluate the degree of dispersion/aggregation of diluted suspensions of milled MZ. Well-dispersed particles give small average particle size d_{50} because particles settle separately. Whereas big aggregates due to flocculation of the particles show higher d_{50} values than for the well-dispersed suspension.

Zeta potential measurements were performed with a model ESA 8000 (Matec Applied Science) through the electroacoustic technique on a 1 vol.% suspension. Zeta potential versus pH curves were determined for milled MZ powder with and without polyacrylate addition.

2.2. Slip casting and characterization of green compacts

Aqueous 37–49 vol.% suspensions at pH 9.1–9.2 were prepared by adding the powder to aqueous solutions with the appropriate amount of dispersant (Dolapix CE64, Zschimmers and Schwartz) and NH_4OH. After mixing, the suspensions were ultrasonically treated.

The apparent viscosity of suspensions as a function of the added amount of dispersant was previously tested to determine the amount required to obtain the minimum viscosity. For the milled MZ powder the optimum amount of dispersant at pH 9 was near to 0.2 wt.%. The addition of approximately 0.25 wt.% of dispersant was required to obtain the optimum dispersion conditions of suspension of the mixture of zircon and α-alumina at pH 9.

Flow curves of concentrated suspensions containing the optimum amount of dispersant were obtained using a rotational viscometer Haake vt550 of coaxial cylinders with NV measure system at 25 °C.

The consolidation of concentrated suspensions by slip casting was carried out in a plaster mould to produce bars of 12 mm × 12 mm × 60 mm which were dried 24 h at room temperature and then at 110 °C up to a constant weight. Density (% of the theoretical) was measured by Hg immersion. The pore size distribution of green samples was measured using Hg porosimetry (Porosimeter 2000, Carlo Erba).

2.3. Sintering

Green probes were sintered up to 1600 °C, using a heating rate of 5 °C/min, and a soaking time of 2 h. Sintered density was determined by the water absorption method. Fired bodies were characterized by XRD (Phillips 3020 goniometer with PW3710 controller, Cu Kα radiation and Ni filter at 40 kV–20 mA). Semi-quantitative crystalline phase composition was calculated by XRD using the Rietveld method. Final microstructures were characterized by SEM-EDAX after polishing and chemical etching.

3. Results and discussion

3.1. Particle size distribution of the materials

Attrition milling of fractionated MZ powder reduced the mean particle size d_{50} from 4 to 0.9 μm. Fig. 1 shows the cumulative fraction finer than diameter CFFD versus particle diameter D curves for milled MZ and their mixtures.

Alumina and zircon powders showed narrow distributions with mean particle sizes d_{50} of 0.4 and 2 μm, respectively. The stoichiometric mixture (d_{50}: 0.9 μm)

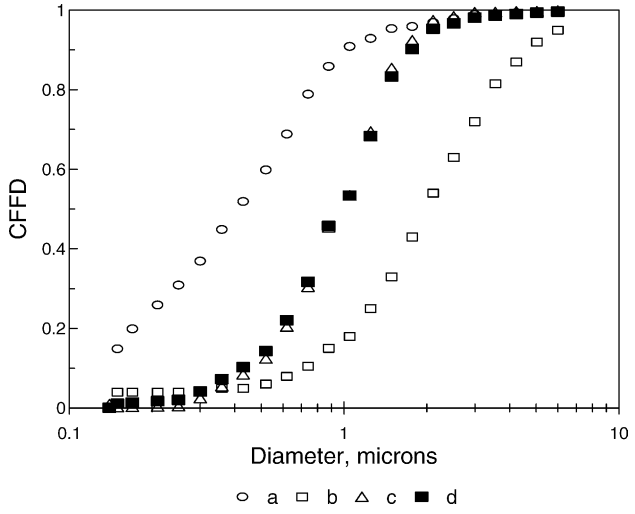

Fig. 1. Cumulative fraction finer than diameter CFFD vs. particle diameter curves. (a) Alumina, (b) zircon, (c) milled MZ, and (d) MZ with 10 wt.% of alumina.

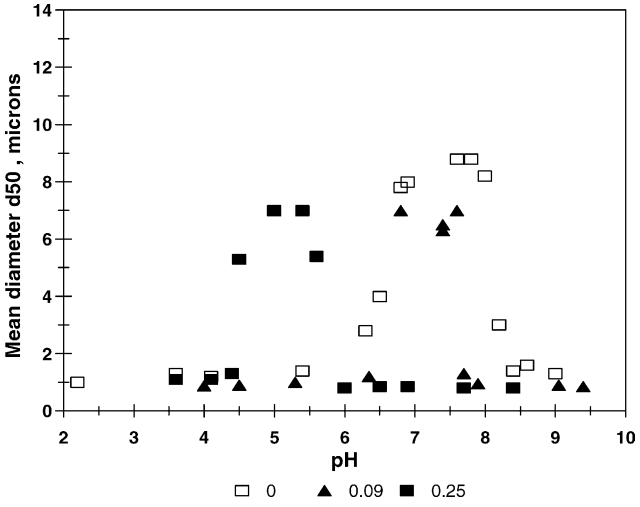

Fig. 3. Mean agglomerate size d_{50} as a function of pH for milled MZ powder with and without different amounts of dispersant.

exhibited a broad particle size distribution. Particle size distribution of milled MZ with addition of 10 wt.% of stoichiometric mixture slightly changed.

3.2. Effect of pH and polyacrylate additions on colloidal stability of diluted suspensions of milled MZ

For the milled MZ powder, zeta potential and average agglomerate size d_{50} measurements were used to determine the colloidal stability of diluted suspensions.

Fig. 2(curve a) shows the variation of zeta potential versus pH for milled MZ powder, this curve indicated that the isoelectric point (iep) was at pH 7. Depending on the pH, the association–dissociation reaction of H^+ with oxide surface groups develop MOH_2^+ or MO^- charged sites (M: Si, Al, Zr). For a pH range above iep the dominant superficial groups are MO^- and thus negative zeta potential increased to −15 mV with increasing pH from 7 to 9.

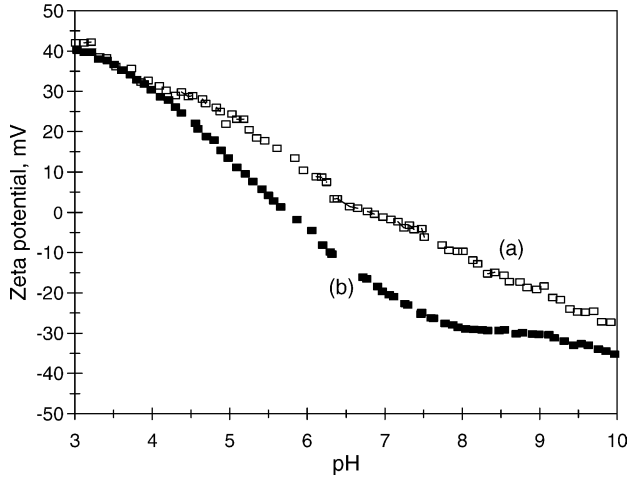

Fig. 2. Zeta potential vs. pH curves. (a) Milled MZ and (b) milled MZ with polyacrylate addition.

According to previous studies through electroacoustic technique the iep of mullite has been determined to be near 7.3 [7–9]. The iep of pure ZrO_2 was reported near to pH 7 [10]. Thus, the iep of the mixture at pH 7 was in agreement with that expected from the reported values for each component.

Fig. 3 shows the variation of the mean particle size d_{50} as a function of pH for milled MZ powder. High d_{50} values near 8 μm were observed at pHs 7–7.5, in accordance with the pH_{iep}, due to the presence of big aggregates resulting from flocculation. In a narrow range of pH, below or above pH_{iep}, d_{50} values decreased to 0.9 μm indicating that degree of dispersion of particles increased. Fig. 2(curve a) shows that below and above pH 7, the magnitude of the zeta potential increased thereby increasing electrostatic repulsion between particles.

Fig. 2(curve b) shows the variation of zeta potential versus pH for milled MZ with polyacrylate addition. The pH_{iep} shifted near pH 5.5 as indicative of anion adsorption. Negative zeta potential increased to −30 mV at pH 9. At pH values higher than 8.5 polyelectrolytes containing carboxylic groups dissociate completely to produce negatively charged anions [11].

The d_{50} values as a function of pH for milled MZ suspensions containing different amounts of dispersant is showed in Fig. 3. For the suspension containing 0.09 wt.% of polyacrylate little effect on the d_{50} values in a pH range from 7.5 to 6.5 was found suggesting low adsorbed amount of dispersant. However, a further increase in polyacrylate concentration to 0.25 wt.% caused important changes in suspension stability. At pH near 5, d_{50} values increased to 7 μm in agreement with a shift in pH_{iep} to 5.5. For a decrease in suspension pH below 4.5, d_{50} decreased to 0.9 μm showing redispersion of particles. Additional negative charges of coated particles were reversed by the presence of more positive surface groups (i.e. positive zeta potentials)

at pHs lower than 4.5. Also, the degree of dissociation of polyacrylate is smaller at pH 6 than that in alkaline media [11] and consequently effectiveness of polyelectrolyte decreases in acidic pHs. From suspension pH between 6.5 and 9.5, d_{50} values reduced. High degree of dispersion of the particles may be explained by an increase of the negative zeta potential (Fig. 2, curve b).

The alkaline range of pH resulting in small mean particle size was relatively wide as compared with that of MZ without polyacrylate adsorbed. This may be attributed to high absolute values of zeta potential. Fig. 2(curve b) shows that negative zeta potential of milled MZ increased from −15 to −30 mV at pH 9 due to specific adsorption polyacrylate anion on powder surface.

Furthermore, at pH 9 adsorption of polyacrylate anion on alumina changed the zeta potential to negative reducing the possibility of heterocoagulation with milled MZ and with zircon which has a high negative zeta potential at this pH [12]. Based on the colloid stability of milled MZ, mixed suspensions with sintering aids may be electrosterically stabilized by polyacrylate adsorption at pH 9.

3.3. Rheological properties of 37–49 vol.% suspensions

The incorporation of fine ceramic powders to MZ suspension was an attempt used to improve flow properties of concentrated suspensions. One difficulty observed has been the adequate dispersion of the MZa and MZaz mixtures as heterocoagulation between components can occur [12,13]. Therefore, polyacrylate addition was necessary to produce well-stabilized suspensions of milled MZ with and without sintering aids.

Fig. 4a–c shows the apparent viscosity versus shear rate curves for milled MZ, MZa, MZaz suspensions, respectively. Stabilized 37 vol.% suspensions of milled MZ and their mixtures having very low viscosity exhibited a shear thinning flow behavior. Apparent viscosity values decreased with increasing shear rate up to a viscosity plateau reached at shear rates higher than 100 s^{-1}.

Viscosity and degree of shear thinning of suspensions decreased with addition of 10 wt.% of sintering aids for high solid contents. Values of viscosity 42 vol.% suspensions were 150 and 50 mPa for milled MZ and MZ with 10 wt.% of sintering aids, respectively. Small particles fitted the interstices between large ones and consequently viscosity of suspensions of MZa relatively decreased due to enhanced particle packing [14,15]. Rheological behavior of suspensions of MZ powder changed to strong shear thickening at shear rates higher 20 s^{-1} with increasing solid content to 49 vol.% (Fig. 4a). This may be related to a narrow particle size distribution and the absence of fine particles, and consequently to a less efficient packing of the particles. Fig. 4b and c shows that viscosity and degree of shear thickening of suspensions decreased with increasing the amount of alumina for high solid contents. Therefore, addition of sintering aids improved flow properties of concentrated suspensions as dilatancy may be deleterious for colloidal processing.

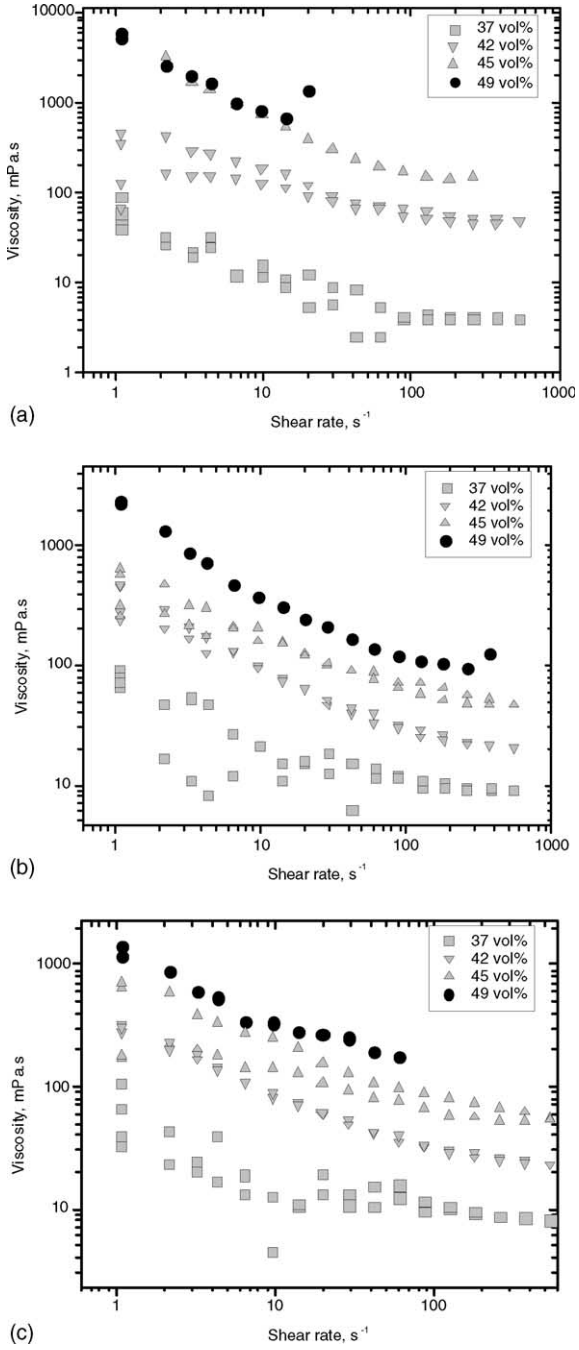

Fig. 4. Viscosity vs. shear rate curves for 37–49 vol.% suspensions with the optimum content of dispersant. (a) MZ, (b) MZa, and (c) MZaz.

3.4. Green density versus solid content

Fig. 5 shows that density of green compacts prepared from 37 vol.% suspension of MZ powders with and without sintering aids achieved 2.47 to 2.40 g/cm^3 (61–59% TD), respectively. Increasing solid concentration up to 45 vol.%, density of compacts prepared from MZa and MZaz

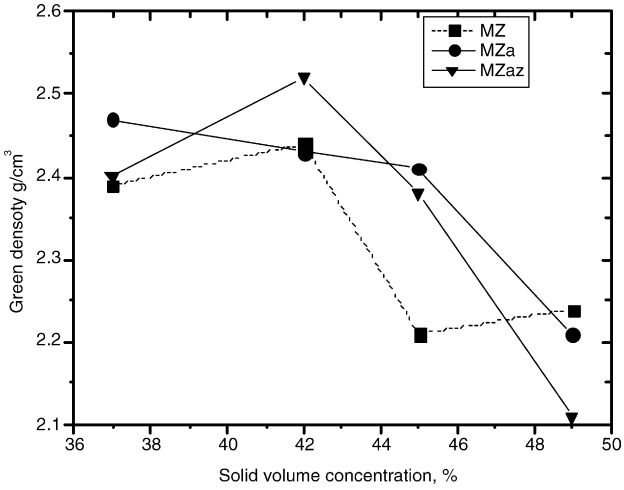

Fig. 5. Green density vs. solid volume concentration for MZ, MZa and MZaz suspensions.

suspensions decreased close to 2.38 g/cm^3 which was higher than 2.20 g/cm^3 for compacts obtained from MZ suspension. This result was attributed to poor packing efficiency due to a narrow PSD of milled powder. Thus, high density was obtained in small range of solid concentration as compared with respective suspensions containing sintering aids.

Micropore size distributions of dried compacts produced by slip casting from 39 vol.% suspension is shown in Fig. 6a. Total pore volume of the compacts decreased with increasing content of alumina in the mixture. Fig. 6b shows that increasing solid content to 45 vol.% viscosity increased as well as green density decreased as a result of high pore volume and size. Differential pore volume curves (not shown) exhibited narrow and unimodal distribution of pores. The most frequent pore radius was 0.035 μm for MZ compacts. As green relative density decreased, pore radius increased to 0.05 μm. However, green compacts remained free of large pores or heterogeneity.

3.5. Phase composition, density and microstructure of the composites

Table 1 shows the crystalline phase composition determined by the Rietveld method. Milled MZ powder was composed by mullite and m-ZrO_2. Tetragonal phase was absent. Very low amounts of unreacted alumina and zircon were identified by XRD. Proportion of m-ZrO_2 were higher than that of the as-receiving MZVr probably due to powder fractionation.

After sintering at 1600 °C, monoclinic zirconia content of the composites slightly decreased whereas t-ZrO_2 proportion increased indicating that the spontaneous transformation t → m which occur on cooling reduced probably due to the fine size of the powder. The ratio of tetragonal to monoclinic zirconia was determined to be low (Table 1). Mullite content in materials prepared from MZa suspensions

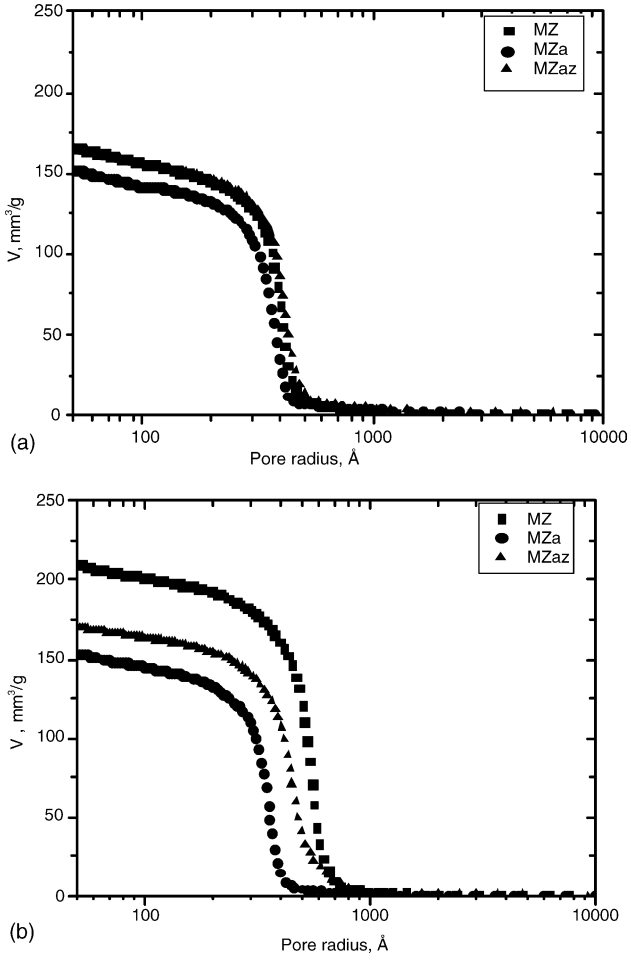

Fig. 6. Cumulative pore size distribution curves for green compacts prepared from milled MZ with and without alumina for 37 and 49 vol.% suspensions.

slightly increased due to mullitization of added alumina. Traces of zircon were detected.

In MZ composites the development of relative high sintered density was mainly controlled by factors such as the phase composition including the relative content of tetragonal and monoclinic zirconia and porosity [5].

Open porosity of sintered materials was approximately 1–2%. No significant differences in sintered density between different compositions used was found. Slightly high density of composites prepared from MZ suspension may be explained by the relatively low mullite content. Addition of alumina enhanced mullitization with a corresponding decrease in density from 3.79 to 3.75 g/cm^3.

Microstructure of the MZ and MZa materials are shown in Fig. 7. Sample MZ (Fig. 7a) shows a homogeneous microstructure of zirconia grains (white) in a mullite matrix. This microstructure do not differ than some mullite–zirconia composites prepared by other authors. Some zirconia grains have an elongated shape because of the raw material employed.

The mullite grains are not clearly defined and low porosity present appeared mainly in the triple points.

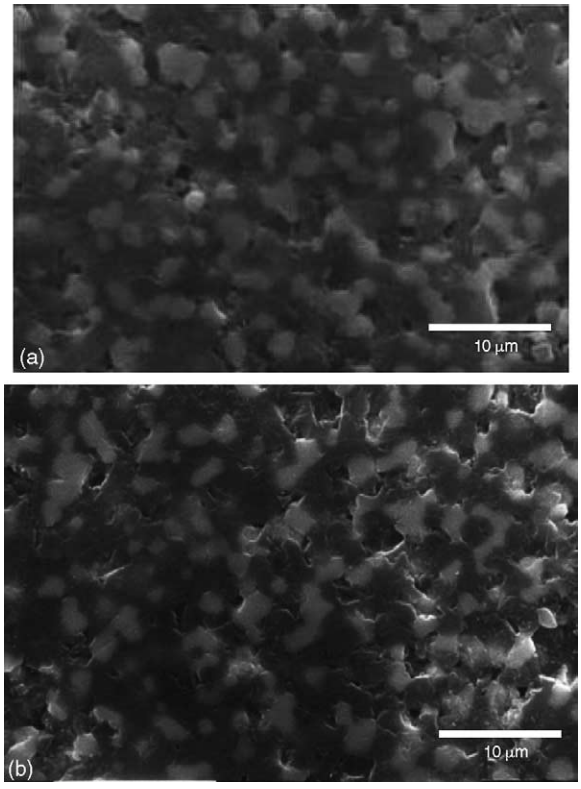

Fig. 7. Microstructure of sintered composites prepared by slip casting from different powders. (a) Milled MZ and (b) MZa mixture.

Microstructure of sample MZa (Fig. 7b) is close to MZ but the matrix is dark due to the higher alumina content than that of MZ. Pore size and distribution are similar to MZ sample.

4. Conclusions

Satisfactory casting 45 vol.% suspensions of milled mullite–zirconia powder with sintering aids were prepared using low amount (0.25 wt.%) of polyacrylate dispersant at pH 9. The low viscosity of mixed suspensions may be related with specific adsorption of polyacrylate on each component. Specific adsorption of polyacrylate anion on the milled MZ powder was evidenced by the pH_{iep} shifting. Addition of 0.25 wt.% of dispersant increased the negative zeta potential to −30 mV at pH 9 higher than that for the milled MZ powder.

Furthermore, adsorption of polyacrylate anion on alumina changed the zeta potential to negative reducing the possibility of heterocoagulation with zircon or MZ powder.

Control of colloid stability by small addition of polyelectrolyte allowed to increased solid content of the suspensions with a suitable flow behavior. Sintering aids improved flow behavior of concentrated suspensions reducing viscosity and dilatancy. Density of green compacts slightly increased with decreasing viscosity of the concentrated suspensions. This may be attributed to a dense packing due to the presence of fine particles. At high solid content, green density decreased as well as increased pore volume and size. However, sintered bodies had a similar density that may be explained by minor differences in phase composition.

References

[1] C. Aksel, F. Komicezny, Mechanical properties and thermal shock behaviour of PSR 333 alumina–mullite–zirconia refractory material, Glass Int. 1 (2001) 16–18.
[2] L. Manfredo, R.N. McNally, The corrosion resistance of high ZrO_2 fusion cast Al_2O_3–ZrO_2–SiO_2 glass refractories in soda lime glass, J. Mater. Sci. 4 (1984) 1272–1276.
[3] H.M. Jang, S.M. Cho, K.T. Kim, Alumina–mullite–zirconia composite. Part II microstructural development and thoughtening, J. Mater. Sci. 2 (1997) 503–511.
[4] N. Claussen, J. Jahn, Mechanical properties of sintered in-situ reacted mullite–zirconia composites, J. Am. Ceram. Soc. (Note) 3/4 (1980) 228–229.
[5] K. Das, S.K. Das, B. Mukherjee, G. Barnerjee, Microstructural and mechanical properties of reaction sintered mullite–zirconia composites with magnesia as additive, Interceram 5 (1998) 304–313.
[6] P. Descamps, S. Sakaguchi, M. Poorteman, F. Cambier, High temperature characterization of reaction sintered mullite–zirconia composites, J. Am. Ceram. Soc. 10 (1991) 2476–2481.
[7] P. Boch, T. Chartier, Tape casting and properties of mullite and zirconia–mullite ceramics, J. Am. Ceram. Soc. 10 (1991) 2448–2452.
[8] N. Ushifusa, M.J. Cima, Aqueous processing of mullite-containing green sheets, J. Am. Ceram. Soc. 10 (1991) 2443–2447.
[9] E. Roncari, C. Galassi, C. Bassarello, Mullite suspensions for reticulate ceramic preparation, J. Am. Ceram. Soc. 12 (2000) 2993–2998.
[10] W.-Ch.J. Wei, S.-Ch. Wang, F.-Y. Ho, Electrokinetic properties of colloidal zirconia particles, J. Am. Ceram. Soc. 12 (1999) 3385–3392.
[11] J. Cesarano, I.A. Aksay, A. Bleier, Stability of aqueous α-Al_2O_3 suspensions stabilized with poly(methacrylic acid) polyelectrolytes, J. Am. Ceram. Soc. 4 (1988) 250–255.
[12] L.B. Garrido, E.F. Aglietti, Zircon based ceramics by colloidal processing, Ceram. Int. 5 (2001) 491–499.
[13] M. Muntean, M. Sparatu, G. Graviliu, Aqueous suspensions of alumina and zirconium silicate mixtures and their rheological behavior, Interceram 2 (2001) 117–119.
[14] J.H.D. Hampton, S.B. Savage, R.A. Drew, Experimental analysis and modeling slip casting, J. Am. Ceram. Soc. 12 (1988) 1040–1045.
[15] P.A. Smith, R.A. Haber, Effect of particle packing on the filtration and rheology behavior of extended size distribution alumina suspension, J. Am. Ceram. Soc. 7 (1995) 1737–1744.